Astronomy & Astrophysics manuscript no. output
March 9, 2020

The Orbital Surface Density Distribution and Multiplicity of M-Dwarfs

N. Susemiehl[1] and M. Meyer[1,]

Department of Astronomy, University of Michigan, Ann Arbor, MI, USA

2019

ABSTRACT

Aims. We present a new estimate of the multiplicity fraction of M-Dwarfs using a log-normal fit to the orbital surface density distribution.
Methods. We used point estimates of multiplicity from five M-Dwarf surveys sampling distinct orbital radii to fit a log-normal function to the orbital surface density distribution of these stars. This model, alongside the companion mass ratio distribution given by Reggiani and Meyer (2013), was used to calculate the frequency of companions over the ranges of mass ratio (q) and semi-major axis (a) that the referenced surveys were collectively sensitive over - [0.60 ≤ q ≤ 1.00] and [0.00 ≤ a ≤ 10,000 AU]. This method was then extrapolated to calculate a multiplicity fraction which encompasses the broader ranges of [0.10 ≤ q ≤ 1.00] and [0.00 ≤ a < ∞ AU]. Finally, the results of these calculations were compared to the multiplicity fractions of other spectral types of stars.
Results. The multiplicity fraction over the constrained regions of [0.60 < q < 1.00] and [0.00 ≤ a ≤ 10,000 AU] was found to be 0.239 ± 0.040. The extrapolated multiplicity fraction over the broader ranges of q (0.10 - 1.00) and a (0.00 - ∞ AU) was calculated as 0.481 ± 0.129. Lastly, the multiplicity of M-Dwarfs is similar to that of FGK and A stars over the constrained regions of mass ratio and semi-major axis.

Key words. binary stars – M-Dwarfs – stellar demographics

1. Introduction

Type M main sequence stars (M-Dwarfs) constitute a majority of nearby stars, comprising as much as 75% of local populations (Henry et. al. 2006). Due to their significant prevalence, it is important to have a deep understanding of the demographics of this type of star. The multiplicity, defined here as the fraction of stars with a gravitationally-bound companion, is an essential value to constrain in this pursuit. Understanding the multiplicity of M-Dwarfs will have important implications for star formation theories, inform us about the emergence of planetary systems around low mass stars, and allow for the modeling of both galactic and extra-galactic stellar populations. Despite these ramifications, the multiplicity fraction of M-Dwarfs is still not yet well-known.

We understand the multiplicity fraction of a sample of stars to be a value that can be numerically estimated using their the companion mass ratio distribution (ψ) and orbital surface density distribution (ϕ). The companion mass ratio distribution represents the fraction of stars which have a companion within a given range of the mass ratio. The mass ratio, q, is defined as the ratio between the masses of the secondary star and primary star where, by definition, the mass of the primary star is greater than that of the secondary star so that $q \leq 1$. The orbital surface density distribution is the fraction of stars which have a companion within a given range of the separation between the two stars. The semi-major axis of an orbital ellipse, a, serves as a measure of the separation between the primary and secondary stars. Integrating either of these functions over specific ranges of their respective parameters returns the fraction of M-Dwarfs which have a binary companion over that range. Therefore, combining the two provides a holistic multiplicity fraction, calculated as:

$$f = \int_{q_{min}}^{q_{max}} \psi dq * \int_{log_{10}a_{min}}^{log_{10}a_{max}} \phi dlog_{10}(a) \quad (1)$$

where $q_{min}, q_{max}, log_{10}a_{min}$, and $log_{10}a_{max}$ represent the lower and upper bounds for the mass ratio and semi-major axis of interest.

Numerous attempts have been made to constrain the multiplicity of M-Dwarfs in the past (e.g. Fischer & Marcy 1992, Janson et. al. 2012, Winters 2019), but none include samples of binary pairs that are complete over the full ranges of mass ratio ($0 < q \leq 1$) or separation ($0 < a < \infty$). Instead, their results are limited to specific sub-populations and are therefore unable to draw conclusions regarding the M-Dwarf population as a whole. This leads to a notable gap in our understanding of these ubiquitous objects.

In order to calculate the multiplicity fraction over any given range of mass ratio and orbital separation, the companion mass ratio and orbital surface density distributions must be known. The companion mass ratio distribution is discussed in Reggiani & Meyer (2013), whose authors find that the power law:

$$\psi = q^{.25\pm0.29} \quad (2)$$

describes this distribution for M-Dwarfs and other types of stars. Here, we attempt to fit the functional form for the orbital surface density distribution. Once this is determined, Equation (1) can be used to calculate the multiplicity of M-Dwarfs by integrating over any given ranges of mass ratio and semi-major axis. This will allow for the computation a total multiplicity estimate for M-Dwarfs.

This method for calculating the multiplicity fraction is built upon a key assumption: that the companion mass ratio distribution does not depend on orbital separation. This assumption allows for the calculation of multiplicity using the separated integral seen in Equation (1). Evidence for it provided by Reggiani & Meyer (2013) and is further discussed in Section 4.3 of this work. Furthermore, the method used in this paper for calculating multiplicity only takes into consideration binary systems and not triplets, quadruplets, etc. This is further discussed in Section 4.4.

In Section 2 of this paper, we describe the methods used to fit the orbital surface density distribution and calculate the multiplicity fraction. In Section 3, the results of the work are presented. In Section 4, we discuss the implications of this work and assumptions that were necessary in completing it.

2. Methods

2.1. The Data

The first step in exploring the orbital surface density distribution and multiplicity of M-Dwarfs was to synthesize point estimates of multiplicity from a variety of different M-dwarf surveys. Data was compiled from surveys which employed the radial velocity (Delfosse et. al. 1998, Fischer and Marcy 1992) and direct imaging (Cortes-Contreras et. al. 2016, Janson et. al. 2012, and Ward Duong et. al. 2015) companion detection methods. This allowed us to investigate companions over a broad range of semi-major axes. Projected separations from the direct imaging surveys are treated as equivalent measures for the distances between the binary pairs as the semi-major axis. Additional surveys utilizing microlensing or astrometry detection methods were not used in this analysis because the radial velocity and direct imaging surveys listed above were found to adequately represent the full range of semi-major axis.

We sought to constrain our analysis to only include detected multiple systems with the values of mass ratio and semi-major axis to which each survey was at least 90% complete. The limiting mass ratio, defined as the value of mass ratio to which all of the five surveys were sensitive, was set by Cortes-Contreras et. al (2016) to 0.60. Each of the other surveys were sensitive to lower values of mass ratio. Any detected multiple system which did not have a mass ratio less than 0.60 was removed from our analysis and those within $0.60 \leq q \leq$ were included. Table (1) gives the point estimate of the multiplicity fraction for each survey along with the respective detection method and range of semi-major axis.

In certain cases, assumptions had to be made about details of the surveys. Delfosse et. al. (1998) reported the period and orbital velocity of stars in their sample, but not the semi-major axis. To remedy this, Kepler's Third Law and the masses of the primaries were used to convert the given values into a semi-major axis. Janson et. al. (2012) did not note the minimum mass ratio that the survey could detect. The authors state: "In every case where $q_m m_a < 0.08\ M_{sun}$, the system is removed from the analysis... Furthermore, we include only stars with primary mass $> 0.2\ M_{sun}$, since lower mass stars are not fully complete out to 52 pc" (Janson et. al. 2012). From this, we took a minimum secondary mass of $0.08\ M_{sun}$ and a minimum primary mass of $0.2\ M_{sun}$ and divided these to reach a limiting mass ratio of 0.4. Both Janson et. al. (2012) and Ward-Duong et. al. (2015) included a small number of multiple systems with K-type primary stars. Each system with a K-type primary was removed from this analysis, and the total sample size number was reduced to only include M-dwarf primaries. Because it covers such a wide range of semi-major axis (3 - 10,000 AU), the data from Ward-Duong et. al. (2015) was split into two bins by orbital separation: 0 - 100 AU and 100 - 10,000 AU. Conducting this split required the assumption that the two populations are independent.

2.2. Fitting the Model

We fit a log-normal model to the orbital surface density distribution of the M-Dwarf multiple systems. This statistical model describes the probability density function the frequency of M-Dwarf binaries as a function of orbital separation via an amplitude (A) which normalizes the model, a mean ($log_{10}(\mu)$) which indicates the peak of the distribution, and a standard deviation ($log_{10}(\mu)$) which describes the spread of the distribution. This model, which we call ϕ, is described by:

$$\phi = A * \frac{e^{-(log_{10}(a)-log_{10}(\mu))^2/(2log_{10}(\sigma)^2)}}{log_{10}(\sigma) * \sqrt{2\pi}} \tag{3}$$

In order to fit the model and find the best values for these parameters, a Markov Chain Monte Carlo (MCMC) routine was utilized. Model frequencies with the test parameters as input were compared to the frequencies from the data using a chi-squared log-likelihood function. Uniform log-priors were chosen with bound $0.0 \leq A \leq 2.0$, $-1.0 \leq log_{10}\mu \leq 2.0$, and $-1.0 \leq log_{10}\sigma \leq 2.0$. The MCMC was initialized with 100 walkers positioned randomly within the bound of the log-prior and ran for 5,000 steps. After this, the flattened chains of each of the three parameters were plotted in order to visualize the convergence of the walkers. This informed the decision to discard the first 200 steps of each flatchain as the burn-in values. The best fit amplitude, mean, and standard deviation were then calculated as the mean value of these chains, with error corresponding to the standard deviation of the respective flatchains. A cornerplot (Figure 1) was produced which shows the distributions of each of the three parameters, and is shown below.

Table 1. Multiplicity Fraction Point Estimates, q > 0.6

Reference	Semi-Major Axis Range (AU)	Primary Mass Range (M_{sun})	Multiplicity Estimate
Delfosse et. al. (1999)	0.00 - 4.63	0.13 - 0.44	0.04 ± 0.018
Fischer & Marcy (1992)	0.04 - 4.00	0.14 - 0.33	0.08 ± 0.034
Cortes-Contreras et. al. (2016)	2.60 - 29.5	0.14 - 0.49	0.07 ± 0.012
Janson et. al. (2012)	3.00 - 227	0.12 - 0.59	0.18 ± 0.016
Ward-Duong et. al. (2015) A	3.00 - 100	0.24 - 0.67	0.11 ± 0.022
Ward-Duong et. al. (2015) B	100 - 10,000	0.32 - 0.52	0.07 ± 0.017

Notes. Table 1. This table depicts each of the M-Dwarf surveys used in this study alongside their respective range of semi-major axis which the survey was at least 90% complete, range of primary star masses, and the point estimate of the multiplicity that we made after excluding companion detections outside the respective semi-major axis range and with q < 0.6.

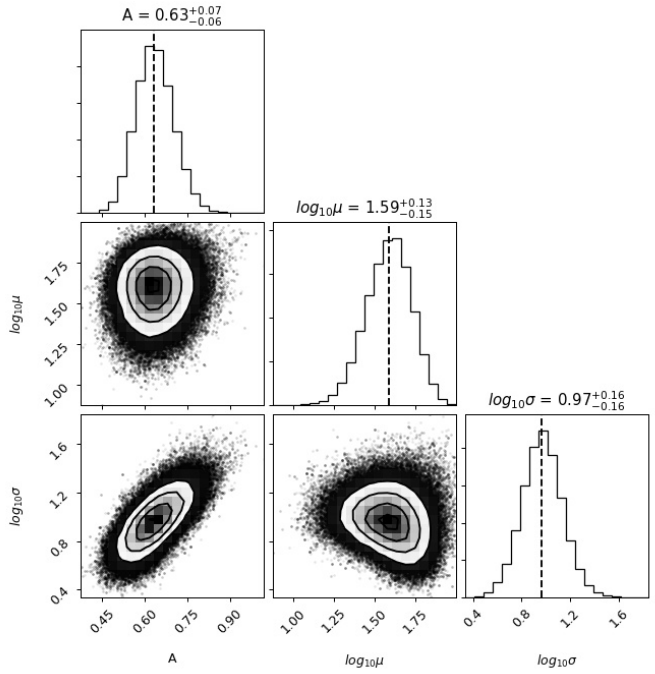

Fig. 1. This cornerplot shows the best fit values with error and marginal distributions of each of the three parameters as well as the covariances between all of them.

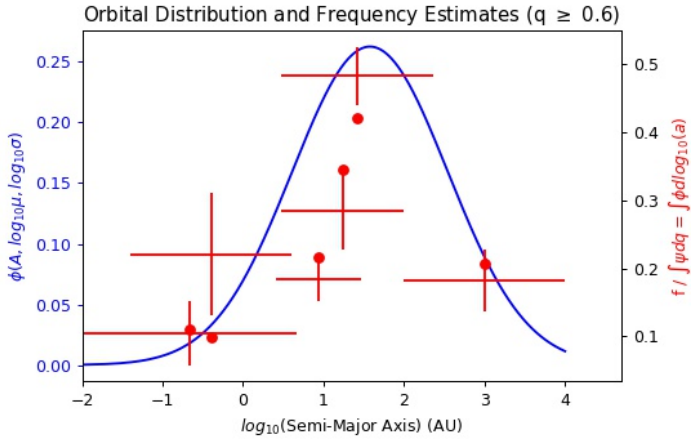

Fig. 2. This figure compares the multiplicity estimates of the source data to estimates made using the fitted model. Each of the red horizontal lines represent one of the six multiplicity estimates from the source data. The right vertical axis position of these lines is the frequency reported in the data (not accounting for the contribution due to the companion mass ratio distribution) and the span along the horizontal axis of these lines is the range in semi-major axis that the respective data covers. The red vertical lines are the error in these multiplicity estimates. The blue curve is the fitted log-normal model of the orbital surface density distribution. Each red dot is the multiplicity estimate (not accounting for the contribution due to the companion mass ratio distribution) obtained by integrating the fitted model over the range. In this figure, multiplicity estimates were depicted only as functions of the orbital surface density distribution and not the second component, the companion mass ratio distribution, in order for a fair comparison to be made between the fitted model and the data. This figure shows a shortcoming of the model as the red dots do not always fall within error of the data estimates.

2.3. Calculating the Frequency

Next, the model for the orbital surface density distribution, with its best-fitting parameters, was used alongside the companion mass ratio distribution model from Reggiani and Meyer (2013) to calculate the multiplicity of M-Dwarfs as:

$$f = \int_{q_{min}}^{q_{max}} q^{.25} dq * A_{best} * \int_{log_{10}a_{min}}^{log_{10}a_{max}} \frac{e^{-(log_{10}(a)-log_{10}(\mu_{best}))^2/(2log_{10}(\sigma_{best})^2)}}{log_{10}(\sigma_{best}) * \sqrt{2\pi}} dlog_{10}(a) \quad (4)$$

This formula was first integrated over the ranges of q and a that encompass the survey data: 0.6 ≤ q ≤ 1.0 and 0.00 ≤ a ≤ 10,000 AU. This calculation resulted in a multiplicity fraction that is representative over these limited ranges of mass ratio and semi-major axis. These ranges were later expanded to [0.10 ≤ q ≤ 1.0] and [0 ≤ a < ∞ AU] to allow for the calculation of a broader M-Dwarf multiplicity fraction. The error on the multiplicity fraction was calculated as the 90% confidence interval of the probability distribution function of the multiplicity fraction. Figure 2 summarizes the model's fit to the data.

3. Results

3.1. Orbital Surface Density Model

The best-fit to point estimates of frequency from the five M-Dwarf surveys resulted in the parameters of A, $log_{10}(\mu)$, and $log_{10}(\sigma)$, being 0.63±0.065, 1.59±0.140, and 0.97±0.16 respectively. This fit is associated with a reduced chi-squared parameter value of 2.143. With three degrees of freedom, the chi-squared probability distribution indicates that the probability of achieving a value greater than or equal to 2.143 is 0.092. Despite this low probability, we do not reject the null hypothesis that the data came from this model.

3.2. Multiplicity Fraction

Integrating Equation (4) over the constrained regions of [0.60 ≤ q ≤ 1.00] and [0 ≤ a ≤ 10,000 AU] resulted in a multiplicity fraction of 0.236 ± 0.061. Following this process, a broad multiplicity fraction was found by integrating Equation (4) over [0.1 ≤ q ≤ 1.0] and [0.0 ≤ a < ∞ AU] to be 0.481 ± 0.129. This broad multiplicity fraction considers stellar and sub-stellar companions to M-Dwarfs, but not planetary companions.

4. Discussion

4.1. Other M-Dwarf Surveys

The results of this work and the multiplicity fraction calculated using the broad ranges of q and a suggest that around half of all M-Dwarfs have a companion. Because this estimate encompasses very small mass ratios, many of these companions may be Brown Dwarfs. We sought to compare our model to the to the prediction of Bowler et. al. (2015), which estimated the frequency of Brown Dwarf companions to M-Dwarf hosts (which translates in this work to a low values of mass ratio). They predict the frequency of Brown Dwarf companions to M-Dwarf primaries over a semi-major axis range of 10 - 100 AU and mass ratio range of 0.039 - 0.224 to be $0.028^{+0.024}_{-0.015}$. We integrated Equation (1) with the best fit parameters described above over these ranges of semi-major axis and mass ratio and obtained an multiplicity estimate of 0.0277 ± 0.0093. The proximity of our results with those of Bowler et. al. (2015) helps enforce the validity of our model. Winters (2019) is another work which describes the orbital surface density distribution and multiplicity of M-dwarfs. They find a peak in the orbital surface density distribution at around 22 AU. This is quite different than our estimate of 39 ± 1.4, but Winters (2019) derived their peak estimate from detections and ignored statistics versus the semi-major axis. An attempt was made to draw a comparison of the multiplicity fraction to Winter (2019). However, the author of this work does not quote the range in mass ratio or the contribution due to binary pairs that correspond to their resulting multiplicity fraction. Therefore, we found it impossible to make an accurate comparison using the previously discussed methods.

4.2. Comparisons to Other Spectral Type Multiplicities

We compare the multiplicity of M-Dwarfs to that of sun-like FGK- and more massive A-type stars over the range of mass ratio and semi-major axis studied here (0.6 ≤ q ≤ 1.0 and 0.00 ≤ a ≤ 10,000 AU). To compare to the FGK multiplicity, we extrapolated the model of orbital surface density from Raghavan et. al. (2010) to integrate over the above range of semi-major axis. This, alongside the companion mass ratio distribution from Reggiani Meyer (2013) described in Equation (2) and the full multiplicity equation, Equation (1), was used to find an FGK star multiplicity fraction of 0.230 ± 0.032, where the error is estimated as the Poisson counting error based on the survey of Raghavan et. al. (2010). We used the same method for the A star multiplicity fraction, this time referencing De Rosa et. al. (2013), and found a multiplicity fraction of 0.238 ± 0.026. Over these ranges, the results are consistent with each other, in contrast to conventional wisdom (Dushene and Kraus 2013)

4.3. On Higher Order Systems

The multiplicity study conducted here was only concerned about the presence of binary systems within the M-Dwarf population. No considerations were made to account for the presence of higher order (triple, quadruple, etc.) systems. While such systems do exist, they are relatively rare. A recent M-Dwarf multiplicity study found that only 3.3% of M-Dwarfs exist as triple and higher order systems (Winters et. al. 2019).

4.4. On the Interdependence of Mass Ratio and Orbital Separation

This work is based on the view that the mass ratio of a stellar binary system does not depend on the separation between its components (Reggiani Meyer 2013). Moe and Di Stefano (2017) found that the distributions of mass ratio and period (which is directly proportional to separation) of systems with O- and B-type main sequence primaries are not independent. Further work exploring the interdependence of mass ratio and orbital separation for specifically type M stars will aid in making a conclusion.

4.5. Summary

We find that the distribution of M-Dwarf binary separations peaks at around 40 AU, which is smaller than the peak for FGK and A stars (Raghavan et. al. 2010). Using this as well as other sources, we find that the multiplicity fraction over [0.60 ≤ q ≤ 1.00] and [0.00 ≤ a ≤ 10,000 AU] for M, FGK, and A stars to be 0.239 ± 0.04, 0.230 ± 0.032, and 0.238 ± 0.026 respectively. We note that these three values are all within error of one-another, suggesting that the multiplicity fraction does not vary strongly with spectral type. Furthermore, we find the multiplicity of M-Dwarfs over 0.10 ≤ q ≤ 1.00 and 0.00 ≤ a ≤ ∞ AU to be 0.481 ± 0.129, predicting the frequency of Brown Dwarf companions to M-Dwarfs to be consistent with Bowler et. al. (2013). Future studies may explore the multiplicity fraction of M-Dwarf companions in the Brown Dwarf regime, explore correlations between the companion mass ratio distribution and separation, as well as compare M-Dwarf multiplicity to L, T, and Y -Dwarf multiplicities.

Acknowledgements. We thank the Formation and Evolution of Planetary Systems group for their consistent support. We also thank Dr. Max Moe and Dr. Kimberly Ward Duong for their insightful advice.

References

Bowler et. al. 2015, The Astrophys. Journal, 216, 1, 7
Cortes Contreras et. al. 2016 , Astro. & Astrophys., FC23
De Rosa et. al. 2013, Mon. Not. R. Astro. Soc. 437, 1216 1240
Delfosse et. al. 1998, Astro. & Astrophys., 344, 897 910
Duchene and Kraus 2013, An. Rev. of Astro. & Astrophys., 51, 1, 269-310
Henry et. al. 2006, The Astrophys. Journal, 132, 2360
Fischer and Marcy 1992, The Astrophys. Journal, 396, 178 194
Janson et. al. 2012, The Astrophys. Journal, 754, 44 70
Moe and Di Stefano 2017, The Astrophys. Journal Supp. Series, 230:15
Raghavan et. al. 2010, The Astrophys. Journal, 190, 1 42
Reggiani and Meyer 2013, Astro. & Astrophys., 553, A124
Ward Duong et. al. 2015, Mon. Not. R. Astro. Soc. 000, 1 34
Winters et. al. 2019, The Astron. Journal, 157, 6